Preparation of ^{99m}Tc-Labeled Iron Oxide Nanoparticles for In Vivo Imaging in Hyperthermia

Sang Hyun Park,* Hui Jeong Gwon, and Sang Mu Choi
Radiation Application Research Division, Korea Atomic Energy Research Institute, Daejeon 305-35, Korea

(Received July 13, 2007; CL-070742; E-mail: parksh@kaeri.re.kr)

^{99m}Tc-Labeled iron oxide nanoparticles ranging in size from 20 to 70 nm were prepared for in vivo imaging in thermotherapy called hyperthermia. The radiolabeled iron oxide nanoparticles were prepared with a high labeling efficiency (over 99%), and they also showed an excellent stability at room temperature for 6 h. This result can give a useful tool for determining the position of the nanoparticles injected into a tissue when hyperthermia treatment is applied in biomedical fields.

Nanoparticles can be used in biomedical applications.[1,2] The possibilities of these applications have drastically increased in recent years.[1–4] In the clinical area of human medicine, these nanoparticles are being used as delivery systems for drugs, genes, and radionuclides.[5,6] They are also attractive for in vitro applications in medical diagnostics, such as research in genetics and technologies based on an immune magnetic separation (IMS) of DNA/RNA, cells, proteins, bacteria, virus, and other biomolecules.[7,8]

Lately, iron oxide nanoparticles are being preferred in clinical studies of cancer therapy because of their excellent magnetic properties and low toxicity for the body system.[1] These iron oxide nanoparticles exposed to an alternating magnetic field can be used for a heat induction that is called hyperthermia which is a heat treatment approach in cancer therapy.[9–11]

Hyperthermia refers to the introduction of ferromagnetic or superparamagnetic particles into a tumor tissue, followed by the application of an external varying magnetic field. The particles transform the energy of the magnetic field into a heat by several mechanisms: eddy current loss, hysteresis loss, and relaxation loss which include a Brownian relaxation and a Neel relaxation.[12] The efficiency of the transformation of energy is strongly dependent on the strength and frequency of the magnetic field, the properties of the magnetic particles, and the cooling capacity of the blood flow.[4] If the temperature exceeds 56 °C, necrosis, coagulation, or carbonization of a tissue is the result; a procedure called "thermoablation."[13,14] For obvious reasons, a thermoablation is only of limited value in clinical applications.[15] In contrast, hyperthermia is highly suitable for cancer therapy, since tumor cells are highly susceptible to elevated temperatures.[16] If tumor cells are heated up to 41–45 °C, the tissue damage for normal tissue is reversible while the tumor cells are irreversibly damaged. This can be an advantage when used in combination with therapies such as radio- and chemotherapy.[14,17] Conventional hyperthermia treatments including microwaves, ultrasound, radiofrequency, and infrared, have already been used successfully. However, their disadvantage is their inability to selectively induce a heat formation in a specific tumor tissue, an inhibition of a heat conduction through a less heat conductive tissue, such as fat and cranial bone, an invasiveness of the methods, and temperature distribution inhomogeneities.[18] Particularly, it was demonstrated that the location of the particles within the cell (intracellular, interstitial, membrane bound) was very important concerning the efficiency of a hyperthermia induction. After removing the hyperthermia induction, most of the nanoparticles could be found in the tumor cells.[19] This is an important problem where the particle is positioned if a hyperthermia treatment is applied.

Radiotracers are widely used nowadays to study a bioavailability, biodistribution, pharmacokinetics, structure–activity relationship, and a receptor-specific binding of novel molecules. This noninvasive imaging approach provides a powerful research tool for the discovery and development of new therapeutic anticancer drugs, providing information which cannot be obtained by other means. ^{99m}Tc is an excellent candidate for a radiodiagnosis because of its ready availability as a carrier-free form from a ^{99}Mo/^{99m}Tc generator. A 6-h half-life and γ-ray emission of 140 keV are appropriate for obtaining a γ-picture.[20]

Therefore, we have prepared ^{99m}Tc-labeled iron oxide nanoparticles using tetrahydroborate exchange resin (BER) as a newly developed reducing agent for determining the position of the nanoparticles injected into a tissue.

The BER was used as a solid-phase reducing agent and an anion scavenger (Figure 1). There are some advantages that the BER is stable in almost all the pH ranges and that it easily removes negatively charged impurities such as unreacted $^{99m}TcO_4^-$ after finishing the reaction by a filtering process. The BER was prepared by the reported method.[21] Chloride-form resin (Amberlite® ion-exchange resin, 12.5 g) was slurry-packed with water into a 30-mL fritted glass funnel mounted on a filter flask. Then, an aqueous sodium borohydride solution (200 mL, 0.25 M) was slowly passed through the resin over a period of 30 min. The resulting resins were washed thoroughly with distilled water until free of excess and finally with ethanol. This resin was analyzed for its borohydride content by a hydrogen evolution upon an acidification with 0.08 M HCl, and the average capacity of BER was found to be 2.5 mequiv of the borohydride ion per gram.

Iron oxide nanoparticles were purchased form Sigma–Aldrich Company (St. Louis, MO, U.S.A.). The labeling efficiency and stability of the ^{99m}Tc-labeled iron oxide nanoparticles were measured with a radio thin layer chromatography (radio-TLC) system which consisted of a radio-TLC scanner (EC & G Berthold Linear Analyzer, Germany) and a one-dimensional analysis of the Berthold chroma program. ^{99m}Tc-Labeled iron oxide nanoparticles solution was spotted onto a silica-gel-coated fiber sheet (Gelman Sciences Inc., Ann Arbor, MI, U.S.A.), and the sheet was eluted with a methylethylketone (MEK) and physio-

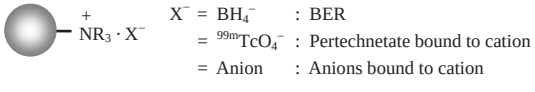

Figure 1. BER as a solid-phase reducing agent and an anion scavenger.

Copyright © 2007 The Chemical Society of Japan

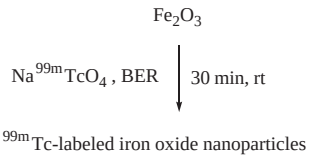

Figure 2. Preparation of the ^{99m}Tc-labeled iron oxide nanoparticles.

Table 1. ITLC analysis of the ^{99m}Tc-labeled iron oxide (^{99m}Tc Fe_2O_3) nanoparticles

Chromatographic System		^{99m}Tc species	
Support	Solvent	Origin	Solvent front
ITLC-SG	MEK	99% of ^{99m}Tc Fe_2O_3	1% of ^{99m}Tc Fe_2O_3
ITLC-SG	Saline	100% of ^{99m}Tc Fe_2O_3	0% of ^{99m}Tc Fe_2O_3

logical saline. The labeling efficiency of the ^{99m}Tc-labeled iron oxide nanoparticles was calculated by comparing the radioactivity of the ^{99m}Tc-labeled iron oxide nanoparticles (at the origin) and the free technetium peaks (at the solvent front).

Experimentally, to a vial containing 5 mg of BER, 0.1 mL of $Na^{99m}TcO_4$ (185 MBq) and a solution of iron oxide (5 mg) in distilled water (0.5 mL) were added at a time, and the mixture was stirred at room temperature for 30 min under N_2 (Figure 2).

To determine the labeling efficiency of the ^{99m}Tc-labeled iron oxide, ITLC-SG (silica gel) was performed by using MEK and saline as a development solvent. The ITLC-SG of the ^{99m}Tc-labeled iron oxide using MEK or physiological saline produced no peak at the solvent front where $^{99m}TcO_4^-$ would be expected. These results indicate that the ^{99m}Tc-labeled iron oxide with a 99% labeling efficiency was formed with the use of BER. The results are given in Table 1. In order to estimate the stability of the ^{99m}Tc Fe_2O_3 nanoparticles, they were stored at room temperature and their radiolabeling efficiency was determined at 1, 2, 4, and 6 h, respectively. The stability was found to be over 98% till 6 h.

The nanoparticles were spotted on to plastic-coated (carbon-stabilized) copper grids (300 mesh) for a characterization by a scanning transmission electron microscope (TEM). The electron micrographs reveal that the Fe_2O_3 nanoparticles were all spherical, and a schematic structure of the nanoparticles is shown in Figure 3.

With regard to the labeling mechanism of the Fe_2O_3 nanoparticle with ^{99m}Tc, we consider that technetium is incorporated onto the surface of the nanoparticle after redox reaction between Tc^{VII} and Fe^{III} and that the final particle size is determined by the initial size of the Fe_2O_3 nanoparticle used.

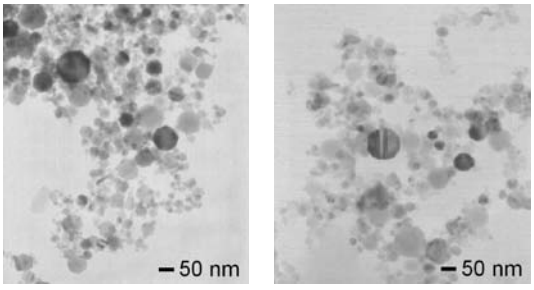

Figure 3. TEM Image scans of the ^{99m}Tc-labeled iron oxide nanoparticles. Left photograph shows the Fe_2O_3 nanoparticles. Right photograph shows the ^{99m}Tc Fe_2O_3 nanoparticles.

In conclusion, the ^{99m}Tc-labeled iron oxide nanoparticles were prepared with a labeling efficiency of 99%. The stability of ^{99m}Tc Fe_2O_3 nanoparticles was also studied, and it was found to be excellent. ^{99m}Tc Fe_2O_3 nanoparticles are found to be very useful for determining of those particle position when the Fe_2O_3 nanoparticles use for local magnetic hyperthermia therapy in tissue.

This work was supported by Korean Ministry of Science and Technology.

References

1 W. Schutt, C. Gruttner, U. Hafeli, *Hybridoma* **1997**, *16*, 109.
2 J. Ugelstad, P. Stenstad, L. Kilaas, *Blood Purificat.* **1993**, *11*, 349.
3 V. Ström, K. Hultenby, C. Gruttner, J. Teller, B. Xu, J. Holgersson, *Nanotechnology* **2004**, *15*, 457.
4 M. Ma, Y. Wu, J. Zhou, Y. Sun, Y. Zhang, N. Gu, *J. Magn. Magn. Mater.* **2004**, *268*, 33.
5 W. Schutt, C. Gruttner, J. Teller, *Artif. Organs* **1999**, *23*, 98.
6 S. S. Davis, *Trends Biotechnol.* **1997**, *15*, 217.
7 F. Scherer, M. Anton, U. Schillinger, J. Henke, C. Bergemann, A. Kruger, B. Gansbacher, C. Plank, *Gene Therapy* **2002**, *9*, 102.
8 O. Olsvik, T. Popovic, E. Skjerve, *Microbiol. Rev.* **1994**, *7*, 43.
9 A. Jordan, R. Scholz, K. Maier-Hauff, F. K. H. van Landeghem, N. Waldoefner, U. Teichgraeber, J. Pinkernelle, H. Bruhn, F. Neumann, B. Thiesen, A. von Deimling, R. Felix, *J. Neurooncol.* **2006**, *78*, 7.
10 M. Johannsen, A. Jordan, R. Scholz, M. Koch, M. Lein, S. Deger, J. Roigas, K. Jung, S. Loening, *J. Endourol.* **2004**, *18*, 495.
11 M. Johannsen, B. Thiesen, A. Jordan, K. Taymoorian, U. Gneveckow, N. Waldofner, R. Scholz, M. Koch, M. Lein, K. Jung, S. A. Loening, *Prostate* **2005**, *64*, 283.
12 B. Hildebrandt, P. Wust, O. Ahlers, *Crit. Rev. Oncol. Hematol.* **2002**, *43*, 33.
13 I. Hilger, W. Andra, R. Hergt, *Radiology* **2001**, *218*, 570.
14 A. Jordan, R. Scholz, K. Maier-Hauff, M. Johannsen, P. Wust, J. Nadobny, H. Schirra, H. Schmidt, S. Deger, S. Loening, W. Lanksch, R. Felix, *J. Magn. Magn. Mater.* **2001**, *225*, 118.
15 A. Jordan, R. Wust, H. Faehling, in *Scientific and Clinical Applications of Magnetic Carriers*, 1st ed., ed. by U. Hafeli, Plenum Press, New York, **1997**, p. 569.
16 M. S. Shinkai, M. Suzuki, S. Iijima, *Biotechnol. Appl. Biochem.* **1994**, *21*, 125.
17 D. C. F. Chan, D. B. Kiprotin, P. A. Brunn, in *Scientific and Clinical Applications of Magnetic Carriers*, 1st ed., ed. by U. Hafeli, Plenum Press, New York, **1997**, p. 607.
18 C. J. Diederich, K. Hynynen, *Ultrasound Med. Biol.* **1999**, *25*, 871.
19 S. Goodwin, C. Peterson, C. Hohn, C. Bittner, *J. Magn. Magn. Mater.* **1999**, *194*, 132.
20 P. H. Marathe, W. G. Humpreys, *Curr. Pharm. Design* **2004**, *10*, 2991.
21 S. H. Park, S. Seifert, H.-J. Pietzsch, *Bioconjugate Chem.* **2006**, *17*, 223.

Published on the web (Advance View) September 27, 2007; doi:10.1246/cl.2007.1282